Journal of Magnetics 27(4), 447-451 (2022)

ISSN (Print) 1226-1750
ISSN (Online) 2233-6656
https://doi.org/10.4283/JMAG.2022.27.4.447

A Study on Image Distortion of 3D-T1-SPACE with Gd Contrast Agent

Yong Soo Han*

Department of Radiological Science, Hallym Polytechnic University, 48, Janghak-gil, Dong-myeon, Chuncheon, Gangwon 24210, Republic of Korea

(Received 3 October 2022, Received in final form 12 December 2022, Accepted 12 December 2022)

In order to increase the qualitative value of MRI and reduce the relative image acquisition time, the mutual intersection of Partial Fourier and Average was conducted to evaluate image distortion and acquisition time according to the effects of FID and Susceptibility Artifact in the T1 3D SPACE Sequence. As a result of analyzing the Roundness (%) of the phantom for Gd contrast agent concentration, when the Partial Fourier 8/8 was fixed, as the Average increased, the Roundness (%) increased (distortion decreased). When the Average 2.0 was fixed, as the Partial Fourier was reduced, the Roundness (%) decreased (distortion increased). As a result of Correlation analysis on Roundness (%), Partial Fourier and Average showed a high positive correlation. Experimental results on image distortion and acquisition time when using the T1 3D SPACE sequence showed that reducing the Partial Fourier than the Average reduced the image distortion and shortened the acquisition time.

Keywords : MRI, SPACE, partial fourier, average, distortion

1. Introduction

Since the treatment effect rate for the small lesions (diameter of 10 mm) of brain metastasis by radiosurgery is considerably high, it is important to conduct accurate diagnosis the brain metastasis in early through Magnetic Resonance Image (MRI) [1, 2]. In recent, the use of sampling perfection with application-optimized contrasts using different flip angle evolutions (SPACE) method have been increased due to the commercialization of high tesla MRI with improved signal to noise ratio (SNR) and spatial/temporal resolution [3]. After obtain gadolinium (Gd) enhanced image, the contrast with the T1 relaxation effect have been increased to reveal even small cell carcinomas, which were difficult to diagnose. However, it has the disadvantage of increasing the scan time [4]. The SPACE uses non-section-selective re-magnetization radio frequency (RF) pulses instead of section-selection re-magnetization pulses [5]. Non-sectioned re-magnetization RF pulses are fast and do not have a sectioned gradient magnetic field. It could obtain echo more than other at the same time [6]. The SPACE has also a higher signal amplitude in the center of the eco train more than obtained with a constant 180° re-magnetization RF pulse, since the SPACE use variable re-magnetization RF pulses less than 180° during the echo train [7].

The acquisition time is most important factor between pulse trains. All methods to increase spatial resolution and SNR accompany increment acquisition time. The more acquisition time after administration of contrast agents, the ability of grasp physiological changes decreases as well as cause of the problem for the increment artifacts in images. In addition, patient processing efficiency also deteriorates, which adversely affects the fiscal of the inspection agency [9-11]. The Partial Fourier Transform (Partial Fourier) and Average during MRI scan usually have been used to adjust the image acquisition time [12, 13]. The Partial Fourier can reduce the image data acquisition time up to 50 % by using the half of the normal number of phase encoding steps [14]. It could maintain the same contrast of tissues during image acquisition time but reduces SNR [15]. In case of the half fourier transform, the SNR is reduced up to 30 % comparing with full phase encoding [16].

The Average could be conducted to improve the SNR and has a meaning of the number of times for each line of K-space data. As the number of Averages increases, several phenomena were accompanied such as increasing signal, reducing noise. These phenomenon could be regarded to be caused by sampling repetition. The SNR

*Corresponding author: Tel: +82-33-240-9355
Fax: +82-33-240-9425, e-mail: hys@hsc.ac.kr

increases by $\sqrt{2}$ when the Average is doubled in proportion to the square root of the volume of each talk and the total number of echoes in the image [17, 18].

In this study, we investigated the characteristics and reduction method of artifacts due to the difference between Partial Fourier and Average for optimization of image acquisition time through Gd phantom scan in T1 3D SPACE sequence using Gd contrast agent.

2. Materials and Methods

2.1. Phantom production

Gadoteridol-based ProHance® (279.3 mg/Ml, 0.5 mol/L) and physiological saline were diluted in a total volume of 3 ml using centrifuge, and the number of 32 phantom were produced for each Gd contrast agent concentration (250, 400, 300, 200, 100, 90, 80, 70, 60, 50, 40, 30, 20, 10, 9, 8, 7, 6, 5, 4, 3, 2, 1, 0.9, 0.8, 0.7, 0.6 , 0.5, 0.4, 0.3, 0.2, 0.1, 0.05 mmol). Using the T1 3D SPACE sequence, in order to know the influence of FID Artifact and susceptibility artifact difference between Partial Fourier and Average, 8 phantoms selected between 10 mmol and 0.1 mmol (10, 8, 6, 4, 2, 0.9, 0.5, 0.1 mmol) in the range of signal strength of 500 or more were evaluated the signal strength and image distortion (Fig. 1).

2.2. Research method

The MRI used in this study was 3T Magnetom Skyra (Siemens, Germany) equipped with head and neck coil for signal collection with 32 Channel. In the T1 3D SPACE Sequence, Average (1.5, 1.7, 1.9, 2.0) was

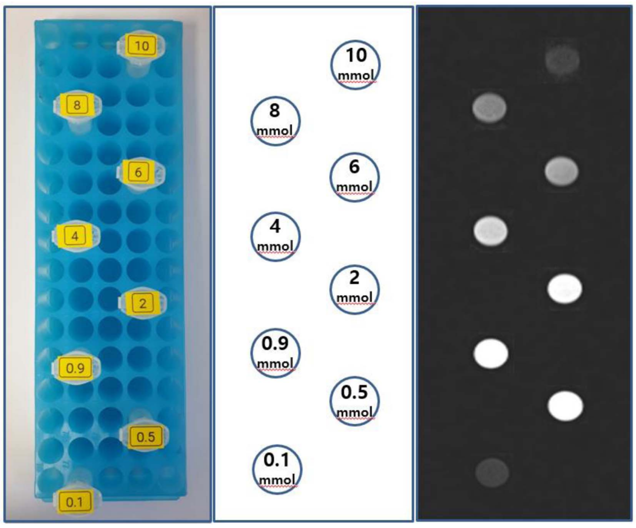

Fig. 1. Phantom and MRI by Gd Contrast Agent Concentration for Image Distortion Evaluation (10, 8, 6, 4, 2, 0.9, 0.5, 0.1 mmol).

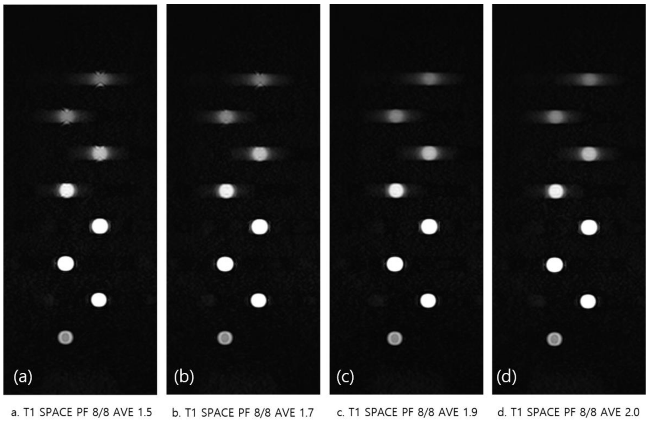

Fig. 2. MR image of T1 3D SPACE Sequence according to Average change (Average : 1.5, 1.7, 1.9, 2.0) in Partial Fourier (8/8).

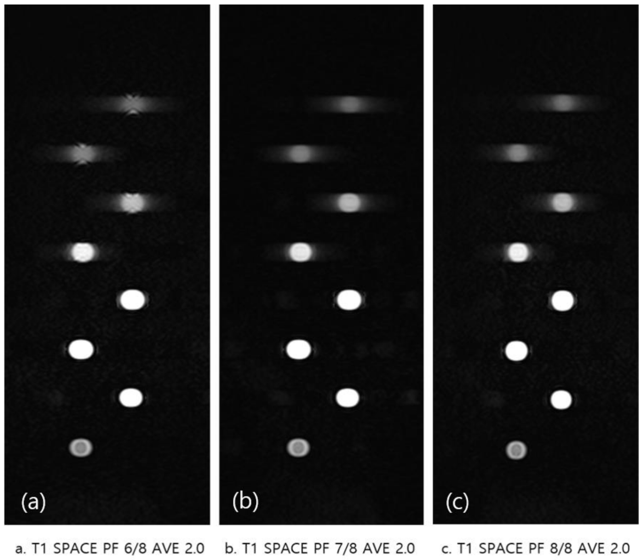

Fig. 3. MR image of T1 3D SPACE sequence according to Partial Fourier change (Partial Fourier : 6/8, 7/8, 8/8) in Average 2.0.

applied based on Partial Fourier (8/8) (Fig.2). In addition, Partial Fourier (6/8, 7/8, 8/8) was applied based on Average 2.0 (Fig. 3). The MRI parameters used in this study are TR: 750 ms, TE: 10 ms, FOV 256 × 256 mm, Matrix 512 × 512, Slice Thickness 0.5 mm, Bandwidth 760 bps, Turbo Factor 52, Echo Train Durations 127 ms and Motion Sensitization Gradients (MSG) was conducted for blood suppression in special preparation module.

2.3. Comparative analysis

The Icy program (ver.1.9.9.0, http://icy.bioimageanalysis.org) was used to measure the signal intensity and the distortion of the image of the contrast agent concentration depending on the variables of Partial Fourier and Average in SPACE. Signal intensity, Roundness (%), and homogeneity obtained through active contours that can extract contours were used for quantitative measurement of distortions due to differences in FID artifacts and magnetization sensitivity. Active Contours are widely used by generating computer curves that find the boundary of medical image, Roundness (%) is a standardized ratio expressed as a percentage (circle or aperture 100 %) between inscribed and circumscribed circles based on ISO 1001 [19]. All statistical process was conducted SPSS version 22.0 (IBM Co., Armonk, NY, USA) and statistical significance p value was get through the Pearson correlation coefficient ($p < 0.05$).

3. Results

We performed the assessment for image distortion acquired according to the values of Partial Fourier and Average to investigate the effect of FID Artifact and Susceptibility Artifact in the T1 3D SPACE Sequence. As a result of analysis for the phantom the Roundness (%) according to the contrast agent concentration, When fix the Partial Fourier 8/8, Increasing Average increased Roundness (%) and decreased distortion (Fig. 4) (Table 1). The Roundness (%) showed the lowest distortion with 0.5mmol at Average 1.5, 1.7 and 0.1mmol at Average 1.9, 2.0. As the Average 2.0 was fixed and the Partial Fourier decreased, the Roundness (%) decreased and the distortion increased (Fig. 5) (Table 2). The Roundness (%) showed the results of highest distortion evaluation with 0.1mmol in Partial Fourier 6/8, 7/8, 8/8. The Roundness (%) had the highest for the image distortion evaluation with an Average of 84.118% at 0.5mmol, and distortion was showed at over 6 mmol with less than 65%.

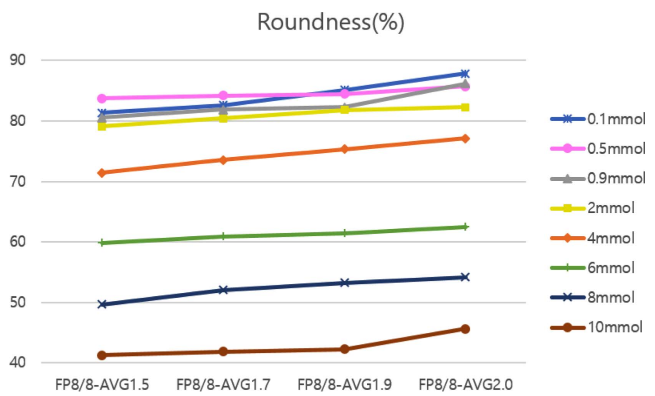

Fig. 4. Roundness (%) change graph of phantom MR images by Gd contrast agent concentration when Average (1.5, 1.7, 1.9, 2.0) is applied based on Partial Fourier (8/8) in T1 3D SPACE Sequence.

Table 1. Roundness (%) change table of phantom MR images by Gd contrast agent concentration when Average (1.5, 1.7, 1.9, 2.0) is applied based on Partial Fourier (8/8) in T1 3D SPACE Sequence.

	FP6/8-AVG2.0	FP7/8-AVG2.0	FP8/8-AVG2.0
mmol	Roundness(%)		
0.1	83.997	85.714	87.838
0.5	82.812	84.299	85.714
0.9	79.541	80.556	86.221
2.0	78.462	80.769	82.264
4.0	70.162	73.585	77.143
6.0	59.777	61.859	62.513
8.0	49.021	50.927	54.167
10.0	40.009	43.214	45.631

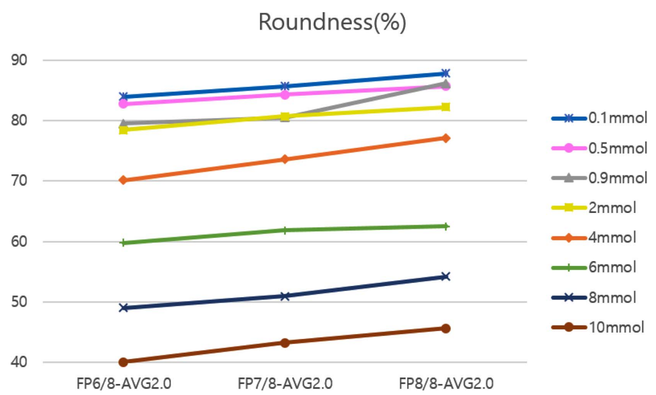

Fig. 5. Roundness (%) change graph of phantom MR images by Gd contrast agent concentration when Partial Fourier (6/8, 7/8, 8/8) is applied based on Average 2.0 in T1 3D SPACE Sequence.

Table 2. Roundness (%) change table of phantom MR images by Gd contrast agent concentration when Partial Fourier (6/8, 7/8, 8/8) is applied based on Average 2.0 in T1 3D SPACE Sequence.

	FP8/8-AVG1.5	FP8/8-AVG1.7	FP8/8-AVG1.9	FP8/8-AVG2.0
mmol	Roundness(%)			
0.1	81.356	82.609	85.106	87.838
0.5	83.750	84.199	84.483	85.714
0.9	80.556	81.905	82.258	86.221
2.0	79.130	80.460	81.818	82.264
4.0	71.429	73.585	75.312	77.143
6.0	59.854	60.937	61.417	62.513
8.0	49.640	52.055	53.261	54.167
10.0	41.250	41.860	42.241	45.631

Table 3. Correlation analysis of Roundness (%) of phantom MR images by concentration of Gd contrast agent by cross experiment of Average and Partial Fourier in T1 3D SPACE sequence.

		0.1 mmol	0.5 mmol	0.9 mmol	2.0 mmol	4.0 mmol	6.0 mmol	8.0 mmol	10.0 mmol
Roundness (%)	Partial Fourier	.959*	.958*	.971*	.959*	.959*	.958*	.971*	.959*
		0	0	0	0	0	0	0	0
	Average	.948	.979*	.963*	.958*	.958*	.979*	.963*	.948
		0	0	0	0	0	0	0	0

**Correlation is significant at 0.01 (two-tailed) level.

As a result of correlation analysis for the Roundness (%) using each factor, Partial Fourier and Average had a high positive correlation (Table 3).

4. Discussion

In general, brain metastasis could be confirmed for the number and size of tumor and location of lesions through contrast-enhanced MRI and the treatment is performed through surgery and external irradiation. Since the effects of radiation irradiation therapy are quite high for the small brain metastases less than 10 mm of diameter, accurate diagnosis for the brain metastasis through MRI in early is very important.

In this reason, the detection of small brain metastases that has a difficult to diagnose by medical images becomes easy, but specific absorption rate (SAR) generated by high magnetic field and low contrast between white matter and gray matter have been shown. The high SAR at 3.0T MRI has a difficult to obtain a T1 3D image, but the development of parameters such as parallel imaging, k-space trajectory and variable flip angle have been solved for that problem.

Kato *et al.* (2009) evaluated the diagnostic performance of T1 3D SPACE and Magnetization Prepared Rapid Gradient Echo (MPRAGE) and usefulness for brain metastasis detection, and Gil *et al.* (2016) conducted the assessment of effectiveness among T1 3D SPACE, 2D FLAIR and 2D T1 Weight Image to detect brain metastasis [20, 21]. Wang *et al.* (2014) also investigated the clinical use of 3D SPACE for the early diagnosis of brain metastases through MRI using Gd contrast agents based on the reason of high treatment rate of brain metastases by radiosurgery [22]. Han *et al.* (2019) studied the changes of signal strength that occur during 3D SPACE scan. However, these existing studies have not been able to solve the problem for the long scan time during 3D SPACE scan and image distortion caused by contrast agents [23]. FID Artifact detects FID signals with echoes due to B1 heterogeneity between the re-magnetization pulse, the spin echo reading interval, incorrected slice profile, and insufficient spoiler gradients. 3D SPACE uses a small and variable re-magnetization flip angle of less than 180°. Especially, it could create a high FID signal for tissues with short T1/T2 time and overlap the echo signal to generate artifacts. The use of Gd contrast agent in the local magnetic field by the difference between two tissues with different susceptibility at interface could be distorted by generating a phase difference of the precession frequency. This might cause increasing and decreasing of magnetic field signal strength out of in phasing when the signal is acquired. In addition, the geometric deformation of the magnetic field might distort the shape of the image and cause an image position dependent error.

Partial Fourier and Average are factors affecting the SNR and image acquisition time according to the method of filling K-space data. We conducted analysis for the distortion evaluation according to Partial Fourier and Average to reduce the scan time in 3D SPACE with high scan effectiveness. The result of evaluation of the distortion was the best with an Average Roundness (%) of 84.12 % at 0.5 mmol. The Roundness (%) was excellent in overall from 0.1 mmol to 2 mmol, 80 %, but it was found that the sharp increase in image distortion appeared at 72.85 % at 4 mmol, 62.30 % at 6 mmol, 51.55 % at 8 mmol, and 42.27 % at 10 mmol, respectively.

Han *et al.* (2019) showed that the signal intensity decreased as the values of the Partial Fourier and Average variables increased through measurements using contrast agents diluted to 4 mmol. In addition, it was also confirmed that the signal intensity decreased as the values of the Partial Fourier and Average variables increased in the dilute contrast medium of 2 mmol or less. The maximum signal strength was found at 0.9 mmol, and the signal intensity and distortions of images that appeared when the image acquisition time was reduced were evaluated using the adjusted Partial Fourier and Average.

In this study, the Partial Fourier 6/8, Average 2.0 and Partial Fourier 8/8, Average 1.5 were set for comparison and evaluation in order to reduce the image acquisition time based on Partial Fourier 8/8 and Average 2.0. The

Roundness (%) of 79.541 % and signal intensity of 1878.85 at Partial Fourier 8/8, Average 2.0 and the Roundness (%) 80.556 % and signal intensity of 2075.80 at Partial Fourier 8/8, Average 1.5 was shown. This means that the maintain of Partial Fourier and decreasing the Average could perform the decrement of image distortion and an increment of signal strength. The highest result of Average distortion according to the contrast agent concentration was at 0.5mmol to 84.118 %.

The limitation of this study was that we were not obtained the results between the various main magnetic fields due to many image distortions occurred by the magnetization-sensitive artifacts of the Gd contrast agent. In addition, as a study limited to the T1 3D SPACE sequence, it could not be to perform comparison with various 3d sequences including such as T1 3D MPRANGE. This suggests the need to proceed with future research.

5. Conclusions

The contrast medium phantom at 0.5 mmol conducted T1 3D SPACE sequence shows the mean Roundness (%) has the lowest image distortion. As a result of performance to reduce the image acquisition time with the T1 3D SPACE sequence, it has been confirmed that the decrease of the Average could conduct the lowest image distortion more than the Partial Fourier. Thus, it will be very helpful for increasing the patient's convenience during MRI scan and diagnosis with the decreasing scan time after use of Gd contrast enhance agent, if the result of above is adapted.

Acknowledgments

This research was supported by the academic research grant from Hallym Polytechnic University in 2021.

References

[1] H. S. Kwak, S. Hwang, G. H. Chung, J. S. Song, and E. J. Choi, Clin. Imaging. **39**, 4 (2015).
[2] E. S. Kim, J. H. Chang, H. S. Choi, J. Kim, and S. K. Lee, AJNR Am J Neuroradiol. **31**, 6 (2010).
[3] S. Lee, W. H. Jee, J. Y. Jung, S. Y. Lee, K. S. Ryu, and K. Y. Ha, Acta Radiol. **56**, 2 (2015).
[4] S. P. Lin and J. J. Brown, J Magn Reson Imaging **25**, 5 (2007).
[5] M. Kitajima, T. Hirai, Y. Shigematsu, H. Uetani, K. Iwashita, K. Morita, M. Komi, and Y. Yamashita AJNR Am J Neuroradiol. **33**, 5 (2012).
[6] J. P. Mugler III, J Magn Reson Imaging **39**, 4 (2014).
[7] R. Busse R., A GE Healthcare MR Publication, Autumn (2007) pp 34-35.
[8] A. Bink, M. Schmitt, J. Gaa, J. P. Mugler III, H. Lanfermann, and F. E. Zanella, Eur Radiol. **16**, 5 (2006).
[9] S. Aime, M. Botta, M. Fasano, and E. Terreno, Chem. Soc. Rev. 27 (1998) 19-29.
[10] L. M. De León-Rodríguez, A. F. Martins, M. C. Pinho, N. M. Rofsky, and A. D. Sherry, J Magn Reson Imaging **42**, 3 (2015).
[11] E. Belorizky, P. H. Fries, L. Helm, J. Kowalewski, D. Kruk, P. R. Sharp, and P. O. Westlund, J Chem Phys. **128**, 5 (2008).
[12] G. McGibney, M. R. Smith, S. T. Nichols, and A. Crawley, Magn Reson Med. **30**, 1 (1993).
[13] M. A. Bernstein, S. B. Fain, and S. J. Riederer, J Magn Reson Imaging **14**, 3 (2001).
[14] J. R. MacFall, N. J. Pelc, and R. M. Vavrek, Magn. Reson. Imaging **6**, 2 (1988).
[15] Y. S. Han, Journal of the Korean Magnetics Society **28**, 5 (2018).
[16] Y. Xu and E. M. Haacke, J Magn Reson Imaging **14**, 5 (2001).
[17] V. G. Kiselev, Magn. Reson. Med. **46**, 6 (2001).
[18] P. Storey, Q. Chen, W. Li, R. R. Edelman, and P. V. Prasad, Magn. Reson. Med. **48**, 6 (2002).
[19] C. W. Bong, C. C. Liew, and H. Y. Lam, Bio-Inspired Computation and Applications in Image Processing (2016) pp 87-104.
[20] Y. Kato, S. Higano, H. Tamura, S. Mugikura, A. Umetsu, T. Murata, and S. Takahashi, AJNR Am J Neuroradiol. **30**, 5 (2009).
[21] B. Gil, E. H. Hwang, S. Lee, J. Jang, H. S. Choi, S. L. Jung, K. J. Ahn, and B. S. Kim, PLoS One **11**, 10 (2016).
[22] J. Wang, Y. Wu, Z. Yao, and Z. Yang, Neuroradiology **56**, 12 (2014).
[23] C. S. Park and Y. S. Han, J Korean Acad Ther **11**, 2 (2019).